CHEMISTRY
A EUROPEAN JOURNAL

DOI: 10.1002/chem.201000282

Hydrolysis of Organophosphate Esters: Phosphotriesterase Activity of Metallo-β-lactamase and Its Functional Mimics

A. Tamilselvi and Govindasamy Mugesh*[a]

Abstract: The phosphotriesterase (PTE) activity of a series of binuclear and mononuclear zinc(II) complexes and metallo-β-lactamase (mβl) from *Bacillus cereus* was studied. The binuclear complex **1**, which exhibits good mβl activity, shows poor PTE activity. In contrast, complex **2**, a poor mimic of mβl, exhibits much higher activity than **1**. The replacement of Cl^- ligands by OH^- is important for the high PTE activity of complex **2** because this complex does not show any catalytic activity in methanol. The natural enzyme mβl from *B. cereus* is also found to be an inefficient catalyst in the hydrolysis of phosphotriesters. These observations indicate that the binding of β-lactam substrates at the binuclear zinc(II) center is different from that of phosphotriesters. Furthermore, phosphodiesters, the products from the hydrolysis of triesters, significantly inhibit the PTE activity of mβl and its functional mimics. Although the mononuclear complexes **3** and **4** exhibited significant mβl activity, these complexes are found to be almost inactive in the hydrolysis of phosphotriesters. These observations indicate that the elimination of phosphodiesters from the reaction site is important for the PTE activity of zinc(II) complexes.

Keywords: enzyme mimics · lactams · organophosphates · structure–activity relationships · zinc

Introduction

Synthetic organophosphorus compounds have been used extensively as pesticides, petroleum additives, and plasticizers.[1] In particular, organophosphorus triesters constitute a major class of crop protectants and their widespread use in agriculture leads to serious environmental problems.[2,3] These compounds are highly toxic to mammals and they affect the nerve system by inhibiting acetylcholine esterase (AChE), a key enzyme involved in the breakdown of acetylcholine.[4] Therefore, degradation of organophosphorus triesters and remediation of associated contaminated sites are of worldwide concern.[5,6] In this regard, the bacterial phosphotriesterase (PTE) enzyme plays an important role in degrading a wide range of organophosphorus esters, including agriculture pesticides, such as paraoxon and parathion, and chemical warfare agents, such as sarin.[7,8]

A comparison of the active site of PTE to that of other binuclear metal-containing enzymes reveals that PTE and the nickel-containing urease have very similar coordination environments around the metal centers.[9] In both the cases, each of the two metal ions is coordinated by two histidine residues from the protein backbone. Whereas an aspartate (Asp) residue is asymmetrically bound to one of the metal ions, a carbamylated lysine and a hydroxide group act as bridging ligands. The distances between two metal centers (Zn···Zn in PTE: 3.4 Å; Ni···Ni in urease: 3.5 Å) are also almost identical. The close structural resemblance of these two proteins suggests that they may have a distant evolutionary relationship.

Recently, Dong et al. have isolated a zinc-containing methyl parathion hydrolase (MPH) from soil-dwelling bacteria that catalyzes the degradation of the organophosphorus pesticide methyl parathion.[10] Interestingly, the active site of MPH has been shown to be very similar to that of metallo-β-lactamase (mβl), which uses a binuclear zinc site (Scheme 1) to hydrolyze the β-lactam ring in penicillins, cephalosporins, and carbapenems. It is, however, not clear whether mβl can hydrolyze organophosphorus triesters. Herein, we show, for the first time, that synthetic zinc(II) complexes that exhibit good mβl activity are poor mimics of PTE and vice versa. We also show that the mβl from *Bacil-*

[a] Dr. A. Tamilselvi, Prof. Dr. G. Mugesh
Department of Inorganic & Physical Chemistry
Indian Institute of Science, Bangalore 560 012 (India)
Fax: (+91) 80-2360-0683/2360-1552
E-mail: mugesh@ipc.iisc.ernet.in

Supporting information for this article is available on the WWW under http://dx.doi.org/10.1002/chem.201000282.

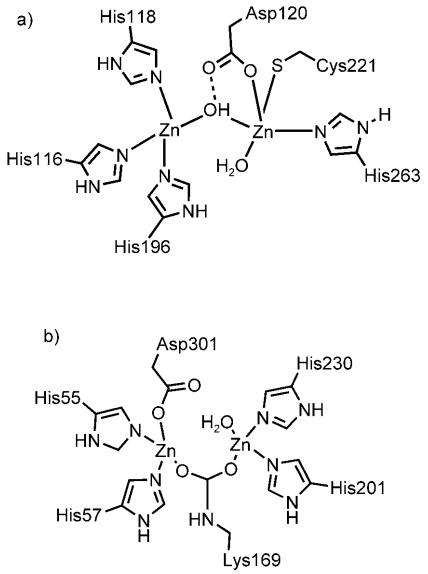

Scheme 1. The chemical structures of the active sites of a) mβl from *Bacillus cereus* (PDB code: 1BC2)[11] and b) PTE from *Pseudomonas diminuta* (PDB code: 1HZY).[12]

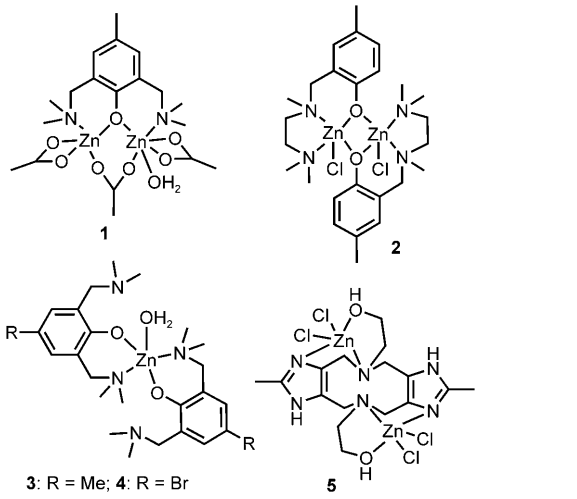

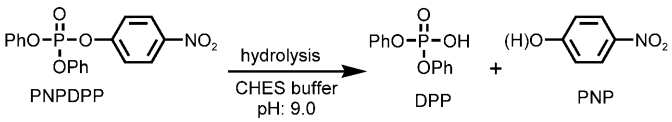

Scheme 2. The hydrolysis of PNPDPP to DPP and *p*-nitrophenol (PNP)[14] in the presence of zinc(II) complexes.

lus cereus is an inefficient catalyst in the degradation of parathion and related compounds.

Results and Discussion

Phosphotriesterase activity of zinc(II) complexes: We have recently reported the metallo-β-lactamase activity of the binuclear complexes **1** and **2** and the mononuclear complexes **3** and **4**.[13] A detailed study of the hydrolysis of β-lactam ring in penicillin and oxacillin mediated by these complexes (**1**–**4**) has revealed the structural requirements for good mβl activity. The binuclear complex **1**, containing a water molecule, exhibited much higher mβl activity than complex **2**, which does not have any water molecules but has labile chloride ligands. We have also shown that the mononuclear complexes **3** and **4** with coordinated water molecules exhibit significant mβl activity. The higher activity of **3** and **4** compared with $Zn(OAc)_2{\cdot}6H_2O$ indicated that the activation of water molecules in complexes **3** and **4** by the *N*,*N*-dimethyl amino group is responsible for their higher catalytic activity. In the present work, we studied the PTE activity of complexes **1**–**5** to understand the correlation between the mβl and PTE activities.

The PTE activity of complexes **1**–**5** was studied by ^{31}P NMR spectroscopy and reverse-phase HPLC methods. In the ^{31}P NMR spectra, the disappearance of signals for the phosphotriester substrate *p*-nitrophenyl diphenylphosphate (PNPDPP) and the appearance of signals for diphenylphosphate (DPP) were followed in CHES buffer at pH 9.0 (Scheme 2). Although complex **1** exhibited excellent mβl activity,[13] this complex showed very poor activity in the hydrolysis of PNPDPP. When complex **1** (20 mM) was added to PNPDPP, a considerable decrease in the peak due to PNPDPP ($\delta = -18.8$ ppm) and an increase in the peak for DPP ($\delta = -12.3$ ppm) was observed (Figure S1 in the Supporting Information). The rate of formation of DPP, however, decreased over a period of time and the reaction did not proceed to completion.

In contrast to complex **1**, the binuclear zinc(II) complex **2**, containing chloride ligands, showed excellent PTE activity. When the reaction was carried out in CHES buffer at pH 9.0, complex **2** efficiently catalyzed the hydrolysis of PNPDPP to produce DPP (Figure 1). After 14 h, the complete disappearance of the peak corresponding to PNPDPP was observed (Figure S2 in the Supporting Information).

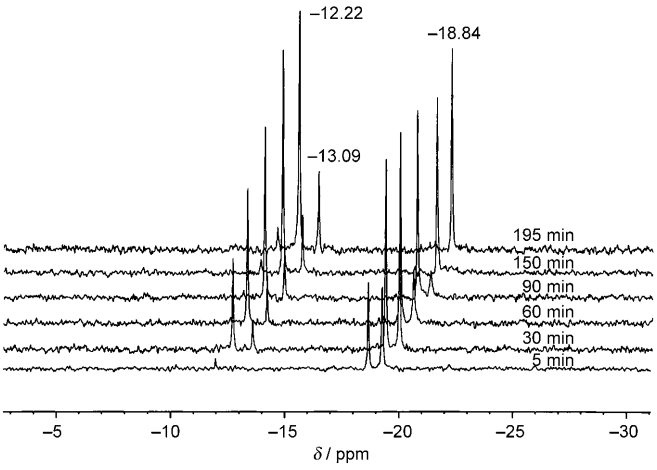

Figure 1. The ^{31}P NMR spectra obtained for the reaction of PNPDPP (20 mM) with complex **2** (20 mM) in CHES buffer (200 mM) at pH 9.0.

The binuclear zinc complex **5**, with two independent zinc(II) centers,[15] exhibited much lower catalytic activity than **2**, however, this complex was found to be a better catalyst than **1** in the hydrolysis of PNPDPP (Figure S3 in the Supporting Information). The mononuclear complexes **3** and **4** did not show any appreciable activity in CHES buffer. It should be noted that complexes **3** and **4** exhibited significant mβl activity in the hydrolysis of β-lactam substrates such as penicillin and oxacillin.[13]

The replacement of the labile chloride ligands by water (hydroxide) ligands appears to be responsible for the PTE activity of complexes **2** and **5**. Although complexes **2** and **5** are quite stable in acetonitrile, they are slowly converted into complexes **6** and **7**, respectively, in aqueous solution, as evidenced by ESI–MS analysis. The protonation state of zinc-bound water/hydroxide, however, depends on the pH of the solution. The formation of binuclear metal complexes with terminal hydroxide ligands has been well documented in the literature.[16]

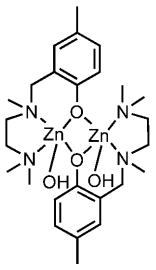

6

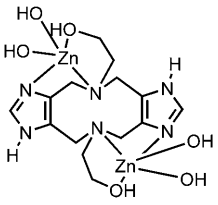

7

Interestingly, complex **1** very effectively catalyzed the cleavage of the P–O bond in PNPDPP in methanol. At room temperature, a complete disappearance of the PNPDPP peak at $\delta = -18.2$ ppm was observed within approximately 300 min (Figure 2). The analysis of the products obtained from the reaction mixture indicated that the signal

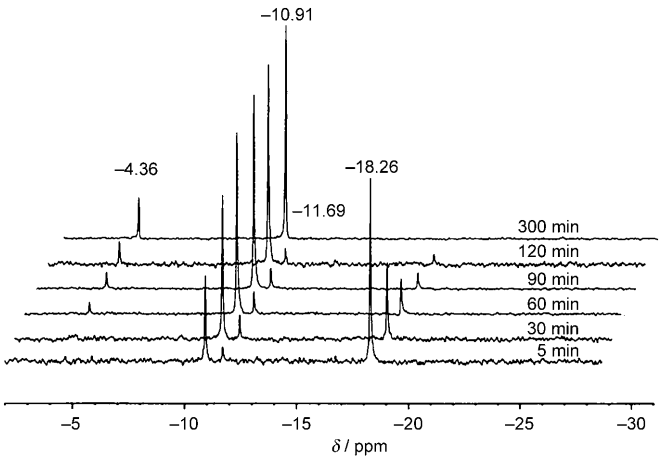

Figure 2. The ^{31}P NMR spectra obtained for the methanolysis of PNPDPP (20 mM) by complex **1** (20 mM).

observed at $\delta = -10.9$ ppm is not due to the hydrolyzed product (DPP), but due to the formation of another phosphotriester, diphenyl methylphosphate (DPMP), by methanolysis as shown in Scheme 3. Brown and co-workers have

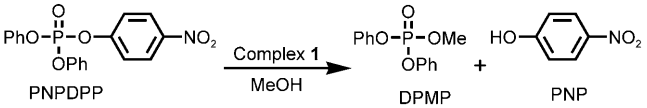

Scheme 3. The methanolysis of PNPDPP to DPMP and *p*-nitrophenol (PNP) in the presence of complex **1**.

shown in a series of studies that the methanolysis of phosphotriesters by transition-metal complexes are generally much faster than the hydrolysis reactions.[17] They have also shown that simple zinc(II) salts, such as $Zn(OTf)_2$ and $Zn(ClO_4)_2$, can efficiently degrade paraoxon and fenitrothion by a methanolysis pathway.[18] Furthermore, alcoholysis reactions have been shown to proceed with different selectivities than hydrolysis. For example, the reactions of some nerve agents with methoxide proceed largely to displace the thiolate group, leading to the formation of the corresponding methoxyesters.[19–20] The selection of substrates for such studies is important because the alcoholysis reactions produce a new phosphotriester instead of a phosphodiester.

In contrast to **1**, complex **2** did not show any noticeable activity when the reaction was carried out in methanol (Figure S4 in the Supporting Information). This is presumably due to the high stability of complex **2** in methanol. Since the zinc-coordinated chloride ligands are intact in methanol, there is no nucleophilic hydroxyl or methoxy group in the complex to cleave the P–O bonds. Complex **2** was also found to be inactive in hydrolyzing PNPDPP when DMSO was used as the solvent. The HPLC and mass spectral analyses indicated that the chloride ligands in **2** remain coordinated to zinc in methanol. The binuclear zinc complex **5**, with two independent zinc(II) centers, was also found to be a relatively poor catalyst in the methanolysis of PNPDPP. Although the chloride ligands in complex **5** are slowly replaced by methoxide (or methanol), only a small amount of PNPDPP was converted to DPMP after 150 min (Figure S5 in the Supporting Information).

In agreement with the ^{31}P NMR spectroscopic experiments, the HPLC data also indicate that complex **2** is more active than complex **1**. The plots of the percentage of PNPDPP versus time for the hydrolysis in the presence of zinc(II) complexes are shown in Figure 3 and the corresponding t_{50} values (the time required for the 50% hydrolysis of the substrate) for PNPDPP are summarized in Table 1. These data indicate that complexes **2** and **5** hydrolyze PNPDPP with t_{50} values of 204.9 and 1282.1 min, respectively, in CHES buffer, and these values are much lower than that of the control reaction ($t_{50} > 4400$ min). Furthermore, the complete hydrolysis of the substrate (100% hydrolysis) was observed with complexes **2** and **5**. The free ligand (2,6-bis[(dimethylamino)methyl]-4-methylphenol)

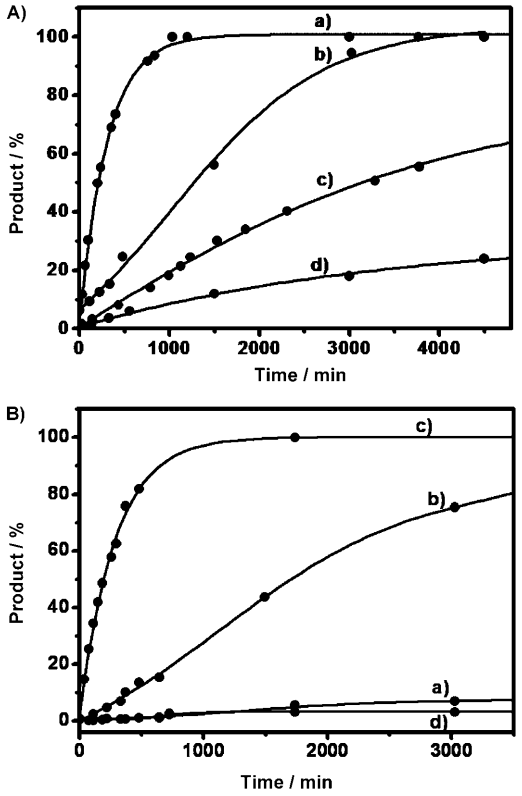

Figure 3. The hydrolysis of PNPDPP (0.20×10^{-3} M) by a) complex **2** (0.21×10^{-3} M), b) complex **5** (0.21×10^{-3} M), c) complex **1** (0.21×10^{-3} M), and d) the control A) ethanol (35%) or B) methanol was used in 20 mM CHES buffer, pH 9.0. To increase the solubility of the PNPDPP in the reaction mixture, The reaction was monitored by reverse-phase HPLC and the amount of *p*-nitrophenol at any given time was calculated from the calibration plot.

Table 1. The t_{50} values and initial rates (v_0) of hydrolysis/methanolysis of PNPDPP by complexes **1**, **2**, and **5** at RT.

Complex	In CHES buffer, pH 9.0		Methanol	
	t_{50} [min][a]	v_0 [μM min^{-1}][c]	t_{50} [min][a]	v_0 [μM min^{-1}][c]
1	3103.0	4.50×10^{-2}	202.8	52.37×10^{-2}
2	204.9	55.89×10^{-2}	> 3026[d]	0.34×10^{-2}
5	1282.1	5.91×10^{-2}	1705.6	3.03×10^{-2}
control	> 4400[b]	1.89×10^{-2}	> 3766[e]	0.15×10^{-2}

[a] The time required for 50% hydrolysis of the substrate (t_{50}) was determined by monitoring the increase in peak area due to *p*-nitrophenol. [PNPDPP]: 0.20×10^{-3} M; [catalyst]: 0.21×10^{-3} M; in EtOH/CHES buffer, pH 9.0. [b] After 4400 min, only 24% hydrolysis was observed. [c] Calculated from the initial 5–10% of the reaction by monitoring the increase in the peak area of *p*-nitrophenol at 23 °C. [d] After 3026 min, only 7% hydrolysis was observed. [e] After 3766 min, only 3.6% hydrolysis was observed.

and $Zn(OAc)_2{\cdot}2H_2O$ did not show any noticeable activity; the initial rates observed in the presence of the ligand and $Zn(OAc)_2{\cdot}2H_2O$ were almost identical to that of the control experiment. The initial rate (v_0) for the hydrolysis of PNPDPP by complex **1** (4.50×10^{-2} μM min^{-1}) was found to be almost ten times lower than that observed for the methanolysis (52.37×10^{-2} μM min^{-1}). For complex **2**, a 164-fold enhancement in the initial rate was observed when the solvent was changed from methanol to buffer (Table 1 and Figure 3). Furthermore, complex **2** was found to be active at concentrations as low as 10 mol% (Figure S6 in the Supporting Information), indicating the catalytic nature of the hydrolysis. The other binuclear zinc(II) complex **5** exhibits good activity both in CHES buffer and methanol, although the rate of hydrolysis in buffer is about two times higher than that of the methanolysis.

Effect of the phosphodiesters on PTE activity: The relatively poor catalytic activity of complex **1** in buffer is probably due to the inhibition of the reaction by the product (DPP). It is possible that DPP can block the zinc(II) coordination sites in complex **1** by forming a bridge between the two metal ions. In such a case, complex **1** cannot bring the hydrolysis reaction to completion once a considerable amount of DPP has been generated in the reaction. It should be noted that Anslyn and co-workers have recently proposed the formation of a phosphodiester-bridged binuclear zinc(II) complex during the transesterification reaction.[21] On the other hand, Lippard and co-workers reported that DPP can bind strongly to binuclear zinc(II) complexes, both as a terminal and as a bridging ligand.[22] To understand the binding of DPP to complex **1**, we carried out the hydrolysis of PNPDPP by complex **1** in the presence of DPP. The reactions were followed by ^{31}P NMR spectroscopy and ESI–MS. The MS analysis of the reaction mixture containing complex **1**, PNPDPP, and DPP indicated the replacement of the bridging acetate ligand in complex **1** by DPP anion leading to the formation of complex **8** (Scheme 4). The ^{31}P NMR

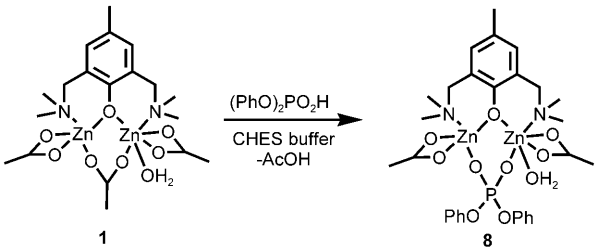

Scheme 4. The formation of the phosphate-bridged binuclear zinc(II) complex **8** by a ligand exchange reaction.

spectrum also indicated the formation of complex **8**. The peak observed for this complex ($\delta=-4.36$ ppm) is shifted downfield compared with that of DPP ($\delta=-12.32$ ppm), indicating that the DPP ligand binds strongly to the binuclear metal center. As the coordination of the DPP ligand in a bridging mode may block the substrate binding, a considerable decrease in the activity was observed upon accumulation of DPP. The spectrum recorded in methanol after 5 h of reaction time, showed only DPMP and small amount of complex **8** (Figure S7 in the Supporting Information). These observations clearly suggest that the low catalytic activity of complex **1** in buffer compared with that in methanol is due to the inhibition by the products formed in the reaction.

The efficient and complete hydrolysis of PNPDPP by complex **2** is unexpected because the hydrolytic reactions of phosphotriesters promoted by transition-metal complexes are not generally catalytic due to the binding of anionic phosphodiesters that inhibit further turnover.[17–20] Although a substantial rate acceleration has been obtained by bridging the binuclear metal centers with two phosphoryl oxygen atoms,[23] a significant product inhibition was observed during the hydrolysis of phosphodiesters by several binuclear zinc(II) complexes. Meyer and co-workers have demonstrated that the hydrolysis of phosphodiesters, such as bis(4-nitrophenyl) phosphate (BNPP), by pyrazolate-based zinc(II) complexes is strongly inhibited by the products.[24] They have also shown that a larger Zn···Zn separation is generally suited for an efficient bridging of phophodiesters.[24b,25] The higher catalytic activity of complex **2** compared with that of **1** in buffer is due to the absence of any significant inhibition by DPP in the reaction catalyzed by complex **2**. The relatively shorter Zn···Zn distance (3.223 Å) and the sterically bulky amino substituents in complex **2** may disfavor a strong binding of DPP at the binuclear zinc(II) center.

To support the conclusions drawn from the NMR spectroscopic experiments, we have studied the effect of DPP on the hydrolysis of PNPDPP by HPLC.[26] When the hydrolysis of PNPDPP by complexes **1** and **5** was carried out in the presence of various concentrations of DPP, a decrease in the activity was observed (Figure 4). In particular, DPP almost

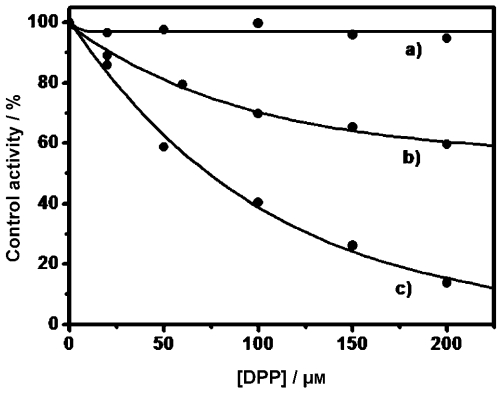

Figure 4. The inhibition of the PTE activity of the binuclear complexes **1** (c), **2** (a), and **5** (b) by DPP in CHES buffer, pH 9.0.

completely inhibited the activity of complex **1** with an IC_{50} value of 73.4 μM. Furthermore, the methanolysis of PNPDPP by complex **1** was also strongly inhibited by DPP (Figure S8 in the Supporting Information) and the inhibition of activity in methanol was found to be similar to that in buffer. A relatively weak inhibition was observed when complex **5** was used as the catalyst. This confirms that the low catalytic activity of complex **1** is mainly due to the strong binding of DPP at the zinc(II) center, as shown in Scheme 4. Interestingly, the hydrolytic activity of complex **2** was unaffected upon treatment with DPP. There was no significant inhibition observed by DPP up to a concentration of 200 μM (Figure 4). These observations indicate that the difference in the activities of complexes **1** and **2** can be attributed to the various degrees of inhibition by the products.

To understand the nature of species produced in the reactions, we have determined the initial rates at different pH values. At low pH values, complex **2** was found to be inactive due to the protonation of Zn−OH species (Figure 5).

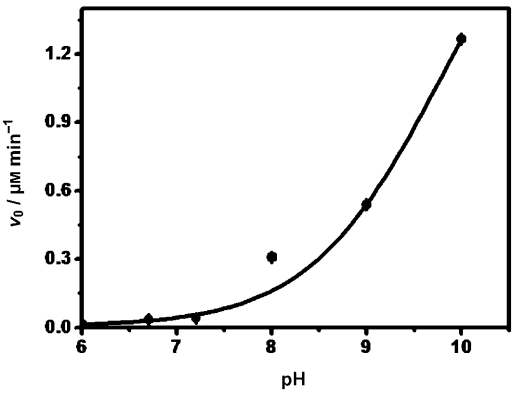

Figure 5. The effect of pH on the reaction rate for the hydrolysis of PNPDPP by complex **2**.

This is in agreement with the report of Samples et al. that the catalytic activity of the binuclear metal site is generally lost upon protonation of the hydroxide bridge at lower pH values.[27] The activity of complex **2** increases drastically with an increase in the pH of the reaction medium. This indicates that the replacement of chloride ligands by hydroxide is responsible for the high catalytic activity. At a pH above 8.0, the conversion of complex **2** to the corresponding hydroxy species **6** takes place rapidly with an increase in the pH. At a pH below 8.0, a considerable amount of protonation takes place, leading to a decrease in the catalytic activity. This is in agreement with the report of Lippard et al. that the rate-limiting nucleophilic attack of the zinc-bound hydroxy species at the substrate, followed by fast protonation of the intermediates leads to the formation of the hydrolyzed products.[28]

Mechanism for the hydrolysis of phosphotriesters by complex 2: Based on the above observations, we proposed the mechanism as shown in Scheme 5 for the hydrolysis of PNPDPP by complex **2**. According to this mechanism, the initial replacement of the chloride ligands in complex **2** by OH^- ligands leads to the formation of complex **6**, which acts as the catalyst in the reaction. Although the binuclear complexes may become mononuclear in solution, the mass spectral data indicate that complexes **2** and **6** do not undergo any dissociation in solution to give the corresponding mononuclear species. An attack of the phosphate group at one of the zinc ions generates the catalyst–substrate complex **9**. As shown by Lippard et al. for the hydrolysis of β-lactams, this binding orients the substrate and the hydroxy group in a fa-

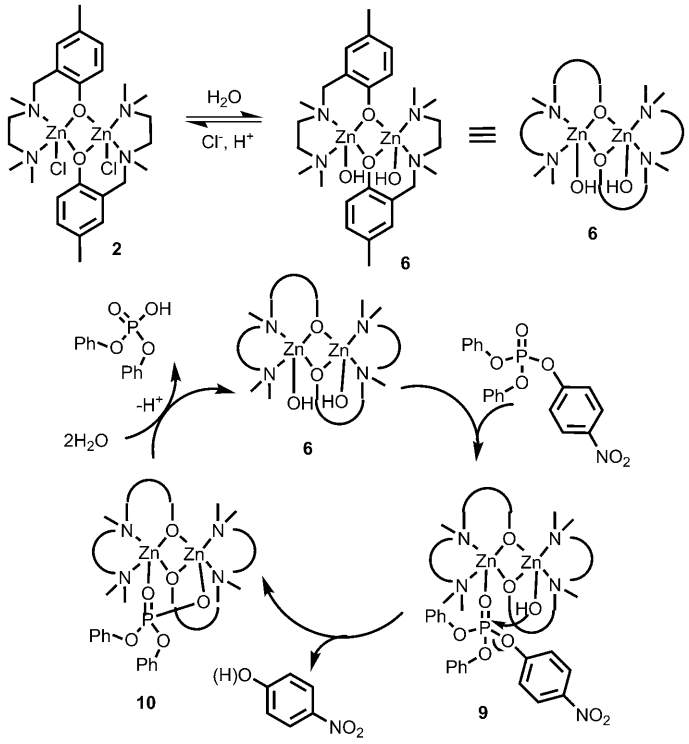

Scheme 5. The proposed mechanism for the hydrolysis of PNPDPP by complex **2**.

vorable position for nucleophilic attack.[29] A signal at $\delta = -13.09$ ppm in the ^{31}P NMR spectrum can be assigned to the catalyst–substrate complex (Figure 1). The formation of complex **9** was also observed in the ESI–MS spectrum. In the second step, the nucleophilic attack of zinc-bound hydroxide at the phosphorus center led to the elimination of *p*-nitrophenol. This results in the formation of complex **10** in which the DPP anion is bridged between two zinc ions. As previously mentioned, this complex is expected to be quite unstable due to the unfavorable binding of the phosphate group. A rapid reaction of complex **10** with water regenerates the catalytically active complex **6**.

A comparison of β-lactamase and PTE activities: To understand the difference in the structural requirement in the zinc(II) complexes for the hydrolysis of phosphotriester and β-lactams, we studied both mβl and PTE activities under identical experimental conditions. A 5:1 mixture of substrate/catalyst was used to keep the reactions under catalytic conditions. Although the mβl activities of complexes **1** and **2** were reported in our previous studies,[13] we have repeated the experiments in CHES buffer at pH 9.0 to ensure that the mβl and PTE activities are obtained under identical experimental conditions (Table 2). A comparison of the t_{50} values obtained for the hydrolysis of oxacillin (β-lactam substrate) and PNPDPP indicates that complexes **1** and **5** exhibit high mβl activity. Interestingly, complex **5**, with two independent zinc(II) centers, was found to be a remarkably efficient catalyst with t_{50} value of 31.0 min. The PTE activities

Table 2. A comparison of β-lactamase and PTE activities of complexes **1**, **2**, **5**, and BcII.

Complex	β-lactamase activity		PTE activity	
	t_{50} [min][a]	v_0 [μM min^{-1}][c]	t_{50} [min][d]	v_0 [μM min^{-1}][h]
1	125.0	9.64	5145.0	0.01
2	2653.0	0.89	220.0	1.73
5	31.4	29.82	>2900[e]	0.19
BcII	364.5	3.69	>2800[f]	0.11
control	>1800[b]	0.09	>2800[g]	0.02

[a] Time required for 50% hydrolysis of oxacillin (t_{50}) was determined by monitoring the decrease in peak area due to oxacillin. [Oxacillin]: 1.0×10^{-3} M; [catalyst]: 0.2×10^{-3} M; in CHES buffer, pH 9.0. [b] After 1800 min, only 29% hydrolysis was observed. [c] Calculated from the initial 5–10% of the reaction by monitoring the decrease in the peak area of oxacillin at 23 °C. [d] Time required for 50% hydrolysis of substrate (t_{50}) was determined by monitoring the increase in peak area due to *p*-nitrophenol. [PNPDPP]: 1.0×10^{-3} M; [catalyst]: 0.2×10^{-3} M; in CHES buffer, pH 9.0. [e] After 2900 min, only 45% hydrolysis was observed. [f] After 2800 min, only 31% hydrolysis was observed. [g] After 2800 min, only 28% hydrolysis was observed. [h] Calculated from the initial 5–10% of the reaction by monitoring the increase in the peak area of *p*-nitrophenol at 23 °C.

of complexes **1** and **5** were, however, extremely low, indicating that the products from the PTE-type reactions show stronger inhibition than those of the mβl reactions. On the other hand, the PTE activity of complex **2** was found to be much higher than the mβl activity of this complex. The t_{50} value obtained for the hydrolysis of PNPDPP by **2** (220 min) was almost ten times lower than that observed for the hydrolysis of oxacillin (2653 min). In contrast, the t_{50} value for the hydrolysis of PNPDPP by complex **5** (>2900 min) was about 100 times higher than that obtained for the hydrolysis of oxacillin (31 min) (Table 2).

As shown in Figure 6A, complex **1** was able to hydrolyze oxacillin completely (100% hydrolysis) within 1500 min, however, this complex hydrolyzed only 20% of PNPDPP during the same period. On the other hand, complex **2** hydrolyzed more than 95% of PNPDPP within 800 min, but the hydrolysis of oxacillin was not complete even after 3000 min (Figure 6B). In contrast to **2**, complex **5** was found to be almost inactive in the hydrolysis of PNPDPP and only approximately 5% conversion was observed after 250 minutes (Figure S9 in the Supporting Information). These observations suggest that the two zinc(II) ions in complex **2** are favorably positioned for the efficient hydrolysis of PNPDPP.

Hydrolysis of PNPDPP by mβl (BcII): In addition to synthetic zinc(II) complexes, we have also studied the PTE activity of mβl from *B. cereus*. Since both mβl and PTE have binuclear zinc active sites, it was thought worthwhile to test the hydrolysis of PNPDPP by mβl. Interestingly, the ^{31}P NMR spectrum indicated that some PNPDPP was rapidly hydrolyzed by mβl to produce DPP (Figure S10 in the Supporting Information), however, after some amount of PNPDPP (ca. 10–15%) had been hydrolyzed, there was no further hydrolysis observed even after 10 h. It was also observed that the amount of DPP produced in the reaction de-

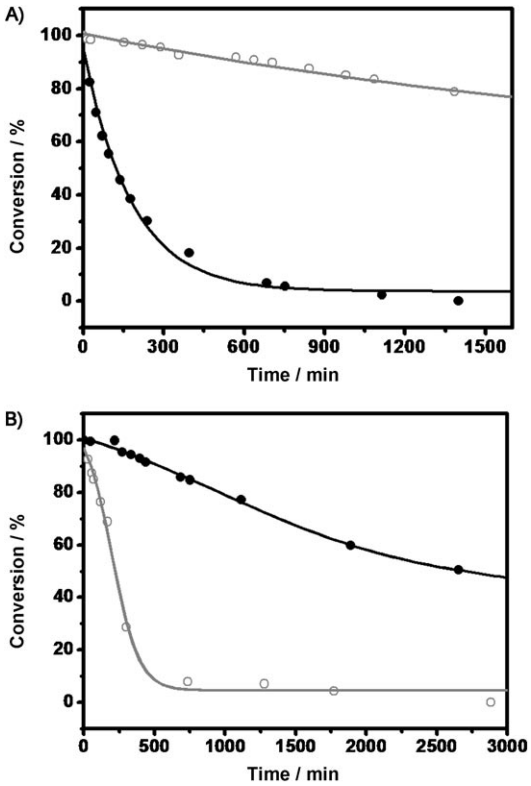

Figure 6. The comparison of PTE (●) and mβl (○) activities of A) complex **1** and B) complex **2**. The hydrolysis experiments were carried out in 20 mM CHES buffer, pH 9.0. For the PTE activity, ethanol (35%) was added to the reaction mixture to maintain the solubility of PNPDPP. The concentrations of oxacillin or PNPDPP were fixed at 1×10^{-3} M and the zinc(II) complexes at 0.2×10^{-3} M.

pends on the concentration of mβl employed for the reactions. These observations suggest that the PTE activity of mβl is significantly inhibited by DPP, which is similar to the inhibition of the PTE activity of complex **1**. We presume that the formation of an enzyme–product complex, as shown in Scheme 6, does not allow the complete hydrolysis of the substrate.

The observations made by ^{31}P NMR spectroscopy are further supported by the HPLC experiments. Whereas the t_{50} value (364.5 min) obtained for the hydrolysis of oxacillin by the enzyme BcII (at 44.4 nM) indicated a facile hydrolysis of

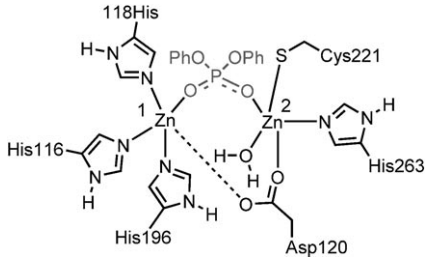

Scheme 6. The possible formation of a stable enzyme–product complex during the hydrolysis of PNPDPP by metallo-β-lactamase from *Bacillus cereus*.

the β-lactam substrate, the t_{50} value could not be obtained for the hydrolysis of PNPDPP even after 1500 min (Figure S11 in the Supporting Information). After this period, only about 20% of the substrate was converted to products. These observations suggest that the presence of the binuclear zinc(II) center is not sufficient to perform efficient hydrolysis of phosphotriesters. The PTE enzyme may follow some interesting mechanisms to eliminate the products, particularly the phosphodiesters, from the active site.

Conclusion

We have shown, for the first time, that the binuclear zinc(II) complexes that exhibit good metallo-β-lactamase (mβl) activity are poor mimics of PTE. A comparison of the PTE activities of bi- and mononuclear zinc complexes indicates that a binuclear metal site is required for the PTE activity. The replacement of Cl^- ligands by OH^- is important for the high PTE activity of complex **2** because this complex is found to be a poor catalyst in methanol. Metallo-β-lactamase from *B. cereus* is found to be an inefficient catalyst in the hydrolysis of phosphotriesters. These observations indicate that the binding of β-lactam substrates at the binuclear zinc(II) center is different from that of phosphotriesters. Furthermore, phosphodiesters, the products from the hydrolysis of phosphotriesters, significantly inhibit the PTE activity of mβl and its functional mimics. This study suggests that binuclear zinc(II) complexes capable of eliminating the products from the catalyst–product complexes would serve as good PTE mimics.

Experimental Section

General procedure: The buffers used for this investigation (MES, pH 5.5–6.4; PIPES, pH 6.5–7.0; HEPES, pH 7.1–8.0; TAPS, pH 8.1–8.9; and CHES, pH 9.0–9.5), diphenyl phosphoryl chloride, diethyl phosphoryl chloride, diethyl thiophosphoryl chloride, and deuterated solvents were purchased from Sigma–Aldrich Chemical Company. HPLC grade solvents were purchased from Merck. Other chemicals, including 2-methyl imidazole, were of the highest purity purchased from local suppliers. All reactions were carried out at room temperature unless otherwise stated. Solvents were purified by standard procedures and were freshly distilled prior to use. ^{1}H (400 MHz), ^{13}C (100.56 MHz), and ^{31}P (161.9 MHz) NMR spectra were obtained on a Bruker 400 MHz NMR spectrometer. Chemical shifts are cited in ppm with respect to $SiMe_4$ as an internal standard (^{1}H and ^{13}C) and phosphoric acid (^{31}P) as an external standard. Mass spectral studies were carried out on a Q-TOF micro mass spectrometer with ESIMS mode analysis as well as in the Bruker ESIMS ion-trap mode. In the case of isotopic patterns, the value given is for the most intense peak. The HPLC experiments were performed on an analytical HPLC system fitted with a PDA detector controlled by EMPOWER software (Waters Corporation, Milford MA). The organophosphates were isolated and purified by using a reverse-phase flash chromatography (Biotage) system.

Synthesis of ligand HL1: This ligand was synthesized by following the method reported in the literature.[15] Ethanolamine (3.05 g, 50 mmol) was added to a solution of 2-methylimidazole (4.11 g, 50 mmol) in water (70 mL). Formaldehyde (8.12 g, 100 mmol, 37% in water) was slowly added and the solution was adjusted to pH 11 with KOH. The reaction

mixture was heated to reflux for 24 h, during which time a suspension was formed. This suspension was filtered and washed with water to yield HL1 as a white solid (7.80 g, 47%). ^{1}H NMR (D_2O/HCl): $\delta = 2.43$ (s, 3H), 3.47 (t, 2H), 3.83 (t, 2H), 4.39 ppm (s, 2H).

Synthesis of 5: Anhydrous $ZnCl_2$ (81.9 mg, 0.6 mmol) was added to a suspension of HL1 (100 mg, 0.3 mmol) in acetonitrile. The reaction was continued for 1 h and the desired product was obtained from the clear solution by crystallization. Crystals suitable for the single-crystal X-ray diffraction studies were obtained by the slow evaporation of the filtrate (73.9 mg, 41%). ^{1}H NMR (CD_3OD): $\delta = 2.29$ (br s, 24H), 3.50 (s, 8H), 7.14 ppm (s, 4H); ^{13}C NMR (CD_3OD): $\delta = 165.3$, 155.1, 130.4, 124.8, 109.4, 101.8, 59.2, 44.2 ppm; MS (ESI): m/z: 534.9 $[Zn_2(HL1)(OH_2)_4]^+$.

Synthesis of PNPDPP: A mixture of diphenyl chlorophosphate (1 mL, 5 mmol), *p*-nitrophenol (0.696 g, 5 mmol), and triethylamine (0.7 mL) in diethyl ether (20 mL) was stirred at room temperature for 12 h. After the completion of reaction, the reaction mixture was poured into water and the compound was extracted from the aqueous layer with diethyl ether. The combined organic fractions were evaporated to dryness to give yellow oil, which was subjected to reverse-phase flash chromatography to give PNPDPP in a pure form (0.156 g, 84%). ^{1}H NMR ($CDCl_3$): $\delta =$ 7.23–7.26 (m, 6H), 7.33–7.40 (m, 6H), 8.24 ppm (d, $J = 9.2$ Hz, 2H); ^{13}C NMR ($CDCl_3$): $\delta = 120.5$, 121.4, 126.3, 126.6, 130.6, 145.6, 150.5, 155.5 ppm; ^{31}P NMR ($CDCl_3$): $\delta = -18.3$ ppm.

Synthesis of parathion: A mixture of diethyl chlorothiophosphate (0.943 mL, 5 mmol), *p*-nitrophenol (0.696 g, 5 mmol), and triethylamine (0.7 mL) in diethyl ether (20 mL) was stirred at room temperature for 12 h. After this period, the reaction mixture was poured into water and the compound was extracted from the aqueous layer with diethyl ether. The combined organic fractions were evaporated to dryness to give yellow oil, which was subjected to reverse-phase flash chromatography to obtain parathion (0.995 g, 68%) in pure form. ^{1}H NMR ($CDCl_3$): $\delta = 1.45$ (t, 6H, $J = 6.8$ Hz), 4.33 (q, $J = 6.8$ Hz, 4H), 7.41 (d, $J = 7.2$ Hz, 2H), 8.30 ppm (d, $J = 7.6$ Hz, 2H); ^{13}C NMR ($CDCl_3$): $\delta = 16.4$, 66.0, 122.1, 125.9, 145.3, 156.0, 188.8 ppm; ^{31}P NMR ($CDCl_3$): $\delta = 62.1$ ppm.

Synthesis of paraoxon: A mixture of diethyl chlorophosphate (0.860 mL, 5 mmol), *p*-nitrophenol (0.696 g, 5 mmol), and triethylamine (0.7 mL) in diethyl ether (20 mL). After stirring the reaction mixture for 12 h at room temperature, the reaction mixture was poured into water and the compound was extracted from the aqueous layer with diethyl ether. The combined organic fractions were evaporated to dryness to give a yellow oil, which was subjected to reverse-phase flash chromatography to obtain paraoxon in a pure form (1.018 g, 74%). ^{1}H NMR ($CDCl_3$): $\delta = 1.38$ (t, $J = 6.8$ Hz, 6H), 4.26 (q, $J = 7.2$ Hz, 4H), 7.39 (d, $J = 9.2$ Hz, 2H), 8.25 ppm (d, $J = 6.8$ Hz, 2H); ^{13}C NMR ($CDCl_3$): $\delta = 16.1$, 65.2, 115.6, 120.6, 125.7, 144.7, 155.6 ppm; ^{31}P NMR ($CDCl_3$): $\delta = -7.0$ ppm.

X-ray crystallography: X-ray crystallographic studies were carried out on a Bruker CCD diffractometer with graphite-monochromatized $Mo_{K\alpha}$ radiation ($\lambda = 0.71073$ Å) controlled by a Pentium-based PC running the SMART software package.[30] Single crystals were mounted at room temperature on the ends of glass fibers and data were collected at room temperature. The structures were solved by direct methods and refined by using the SHELXTL software package.[31] All non-hydrogen atoms were refined anisotropically, and hydrogen atoms were assigned idealized locations. Empirical absorption corrections were applied to all structures by using SADABS.[32]

Crystal data for 5: $C_{16}H_{30}Cl_4N_6O_4Zn_2$; $M_r = 643.00$; monoclinic; space group $P2_1/n$; $a = 7.7441(13)$, $b = 13.369(2)$, $c = 12.092(2)$ nm; $\alpha = 102.841(3)°$; $V = 1220.6(4)$ Å^3; $Z = 2$; $\rho_{calcd} = 1.750$ g cm^{-3}; $Mo_{K\alpha}$ radiation ($\lambda = 0.71073$ Å); $T = 293(2)$ K; $R_1 = 0.0441$ ($I > 2\sigma(I)$); $wR_2 = 0.1277$ (all data). Further details about the crystal structures can be obtained from the CCDC.[33]

Hydrolysis of PNPDPP, parathion, and paraoxon: The hydrolysis reactions of PNPDPP, paraoxon, and parathion were followed by ^{31}P NMR spectroscopy. All NMR spectroscopic experiments were carried out at 293 K. The chemical shifts are given in ppm relative to phosphoric acid as an external reference. In each experiment, the test solution contained 20 mM of complex and 20 mM of PNPDPP, paraoxon, or parathion. The experiments were carried out in either CHES buffer (200 mM, pH 9.0) or in methanol and the progress of the reaction was followed with respect to time.

Determination of β-lactamase and phosphotriesterase activities: The kinetics of the hydrolysis of PNPDPP was followed by HPLC with a reverse-phase column. All reactions were carried in methanol or in CHES buffer (0.02 M pH 9.0). The stock solutions of test complexes, PNPDPP, and oxacillin were prepared in the appropriate solvent and used immediately for the experiments to avoid any possible decomposition. The concentrations of stock solutions of PNPDPP, oxacillin, and the complexes were fixed at 10×10^{-3} M. In a typical kinetic experiment, a sample vial containing the test complexes (1.5 mL) with the appropriate concentration of PNPDPP or oxacillin was incubated. At various time intervals, aliquots (10 μL) were removed from the reaction mixture and injected directly onto the HPLC column. In the case of β-lactamase activity, the compounds were eluted in a linear gradient mode with a mixture of 30–80% acetonitrile and 0.1% TFA over 8.5 min at a flow rate of 1.0 mL min^{-1}. The reaction product (oxacillin turnover product, retention time: 3.66 min) and oxacillin (retention time: 4.24 min) were separable by column chromatography. The chromatograms were extracted at 254 nm and the concentration of oxacillin or the hydrolyzed product was determined for each injection from the peak area by using a calibration plot. In the case of phosphotriesterase activity, the compounds were eluted in an isocratic mode with a mixture of 80% methanol and 0.1% TFA in water over 6.5 min at a flow rate of 1.0 mL min^{-1}. The reaction product *p*-nitrophenol (retention time: 3.78 min) and PNPDPP (retention time: 5.27 min) were separable on a column. The chromatograms were extracted at 305 nm and the concentration of *p*-nitrophenol was determined for each injection from the peak area by using a calibration plot. To avoid any significant changes in the concentrations of the starting materials only the first 5–10% of conversion was followed in most of the cases. To calculate the percentage conversion in the presence of the enzymes and complexes, the test samples were injected onto the column at regular time intervals.

Acknowledgements

This study was supported by the Department of Science and Technology (DST), New Delhi, India. G.M. acknowledges the DST for the award of Ramanna and Swarnajayanti fellowships and A.T. thanks the University Grants Commission (UGC) for a research fellowship.

[1] J. Dragun, A. C. Kuffner, R. W. Schneiter, *Chem. Eng.* **1984**, *91*, 65–70.
[2] D. B. Barr, R. Bravo, G. Weerasekera, L. M. Caltabiano, R. D. Whitehead, A. O. Olsson, S. P. Caudill, S. E. Schober, J. L. Pirkle, E. J. Sampson, R. J. Jackson, L. L. Needham, *Environ. Health Perspect.* **2004**, *112*, 186–200.
[3] a) B. E. Mileson, J. E. Chambers, W. L. Chen, W. Dettbarn, M. Ehrich, A. T. Eldefrawi, D. W. Gaylor, K. Hamernik, E. Hodgson, A. G. Karczmar, S. Padilla, C. N. Pope, R. J. Richardson, D. R. Saunders, L. P. Sheets, L. G. Sultatos, K. B. Wallace, *Toxicol. Sci.* **1998**, *41*, 8; b) J. E. Casida, G. B. Quistad, *Chem. Res. Toxicol.* **2004**, *17*, 983–998.
[4] M. Lotti, *Toxicology* **2002**, *181*, 245–248.
[5] a) Food and Agriculture Organization. The Ticking Time Bomb: Toxic Pesticide Waste Dumps; News Highlights, **2001**, http://www.fao.org/News/2001/010502-e.htm; b) Food and Agriculture Organization. Prevention and Disposal of Obsolete Pesticides, **2001**, http://www.fao.org/WAICENT/FAOINFO/AGRICULT/AGP/AGPP/Pesticid/Disposal/index_en.htm.
[6] S. Bird, T. D. Sutherland, C. Gresham, J. Oakeshott, C. Scott, M. Eddleston, *Toxicology* **2008**, *247*, 88–92.
[7] a) G. Amitai, R. Adani, G. Sod-Moriah, I. Rabinovitz, A. Vincze, H. Leader, B. Chefetz, L. Leibovitz-Persky, D. Friesem, Y. Hadar, *FEBS Lett.* **1998**, *438*, 195–200; b) N. Sethunathan, T. J. Yoshida,

Microbiology **1973**, *19*, 873–875; c) C. M. Serdar, D. T. Gibson, D. M. Munnecke, J. H. Lancaster, *Appl. Environ. Microbiol.* **1982**, *44*, 246–249; d) H. Shim, F. M. Raushel, *Biochemistry* **2000**, *39*, 7357–7364.
[8] B. K. Singh, *Nat. Rev. Microbiol.* **2009**, *7*, 756–764.
[9] E. Jabri, M. B. Carr, R. P. Hausinger, P. A. Karplus, *Science* **1995**, *268*, 998–1004.
[10] Y.-J. Dong, M. Bartlam, L. Sun, Y.-F. Zhou, Z.-P. Zhang, C.-G. Zhang, Z. Rao, X.-E. Zhang, *J. Mol. Biol.* **2005**, *353*, 655–663.
[11] S. M. Fabiane, M. K. Sohi, T. Wan, D. J. Payne, J. H. Bateson, T. Mitchell, B. Sutton, *Biochemistry* **1998**, *37*, 12404–12411.
[12] M. M. Benning, H. Shim, F. M. Raushel, H. M. Holden, *Biochemistry* **2001**, *40*, 2712–2722.
[13] A. Tamilselvi, M. Nethaji, G. Mugesh, *Chem. Eur. J.* **2006**, *12*, 7597–7606.
[14] The bright yellow color developed during the reaction indicates that PNP is largely deprotonated at pH 9.0.
[15] The crystal structure of complex **5** is almost identical to that of the related Cu^{II} complex reported: W. L. Driessen, D. Rehorst, J. Reedijk, I. Mutikainen, U. Turpeinen, *Inorg. Chim. Acta* **2005**, *358*, 2167–2173.
[16] a) S. Albedyhl, D. Schnieders, A. Jancsó, T. Gajda, B. Krebs, *Eur. J. Inorg. Chem.* **2002**, 1400–1409; b) H. Arii, Y. Funahashi, K. Jitsukawa, H. Masuda, *Dalton Trans.* **2003**, 2115–2116; c) G. Yang, R. Miao, Y. Li, J. Hong, C. Zhao, Z. Guo, L. Zhu, *Dalton Trans.* **2005**, 1613–1619.
[17] a) T. Liu, A. A. Neverov, J. S. W. Tsang, R. S. Brown, *Org. Biomol. Chem.* **2005**, *3*, 1525–1533; b) S. A. Melnychuk, A. A. Neverov, R. S. Brown, *Angew. Chem.* **2006**, *118*, 1799–1802; *Angew. Chem. Int. Ed.* **2006**, *45*, 1767–1770; c) D. R. Edwards, G. E. Garrett, A. A. Neverov, R. S. Brown, *J. Am. Chem. Soc.* **2009**, *131*, 13738–13748.
[18] W. Desloges, A. A. Neverov, R. S. Brown, *Inorg. Chem.* **2004**, *43*, 6752–6761.
[19] a) Y.-C. Yang, J. A. Baker, J. R. Ward, *Chem. Rev.* **1992**, *92*, 1729–1743; b) Y.-C. Yang, *Acc. Chem. Res.* **1999**, *32*, 109–115.
[20] Y.-C. Yang, F. J. Berg, L. L. Szafraniec, W. T. Beaudry, C. A. Bunton, A. Kumar, *J. Chem. Soc. Perkin Trans. 2* **1997**, 607–613.
[21] K. Worm, F. Chu, K. Matsumoto, M. D. Best, V. Lynch, E. V. Anslyn, *Chem. Eur. J.* **2003**, *9*, 741–747.
[22] T. Tanase, J. W. Yun, S. J. Lippard, *Inorg. Chem.* **1996**, *35*, 3585–3594.
[23] J. Chin, *Curr. Opin. Chem. Biol.* **1997**, *1*, 514–521.
[24] a) B. Bauer-Siebenlist, F. Meyer, E. Farkas, D. Vidovic, J. A. Cuesta-Seiji, R. Herbst-Irmer, H. Pritzkow, *Inorg. Chem.* **2004**, *43*, 4189–4202; b) B. Bauer-Siebenlist, F. Meyer, E. Farkas, D. Vidovic, S. Dechert, *Chem. Eur. J.* **2005**, *11*, 4349–4360.
[25] F. Meyer, *Eur. J. Inorg. Chem.* **2006**, 3789–3800, and references therein.
[26] Diphenyl phosphate (DPP) required for the inhibition study was generated in situ by adding diphenyl phosphoryl chloride (DPPC) to CHES buffer at pH 9.0. When DPPC was added to the buffer, rapid hydrolysis took place and the quantitative formation of DPP was observed. This conversion can be easily followed by ^{31}P NMR spectroscopy. When DPPC was added to the buffer, the peak at $\delta = -5.1$ ppm for DPPC disappeared completely to produce a new signal at $\delta = -11.9$ ppm for DPP.
[27] C. R. Samples, T. Howard, F. M. Raushel, V. J. DeRose, *Biochemistry* **2005**, *44*, 11005–11013.
[28] N. V. Kaminskaia, C. He, S. J. Lippard, *Inorg. Chem.* **2000**, *39*, 3365–3373.
[29] N. V. Kaminskaia, B. Spingler, S. J. Lippard, *J. Am. Chem. Soc.* **2000**, *122*, 6411–6422.
[30] SMART, version 5.05, Bruker AXS: Madison, **1998**.
[31] a) SHELXTL, V97–2, G. M. Sheldrick, Siemens Industrial Automation Inc., Madison, **1997**; b) SHELX-97, Program for crystal structure solution and refinement, G. M. Sheldrick, University of Göttingen, Göttingen (Germany), **1997**.
[32] SADABS, Version 2, Multi-Scan Absorption Correction Program, G. M. Sheldrick, University of Göttingen, Göttingen (Germany), **2001**.
[33] CCDC-764156 contains the supplementary crystallographic data for this paper. These data can be obtained free of charge from The Cambridge Crystallographic Data Center via www.ccdc.cam.ac.uk/data_request/cif.

Received: February 2, 2010
Published online: June 23, 2010

